KINEMATIC-WAVE FURROW IRRIGATION MODEL

By Wynn R. Walker[1] and Allan S. Humpherys,[2] Members, ASCE

ABSTRACT: A kinematic-wave model of furrow irrigation under both continuous and surged flow management was developed and verified. Numerical solution of the differential continuity equation is accomplished with a Eulerian first-order integration coupled with the assumption that flow rate and flow area are uniquely related by the Manning uniform flow equation. Field data from three Colorado sites, a Utah site, and an Idaho site were used to verify the model's continuous flow simulation of advance and recession. The sites represented a wide range of soil types, field slopes and lengths, and duration of the irrigation event. Companion data from the Utah and Idaho sites were used to verify the model's analysis of surge flow conditions.

INTRODUCTION

Mathematical models of surface irrigation processes can be generally classified as: (1) Hydrodynamic (1,9,10); (2) zero-inertia (6,19); (3) kinematic-wave (3,12,15,18); and (4) volume balance (7,11). Most models were developed for border irrigated conditions and later modified for basin and furrow systems (6,7,11,17,20).

Furrow simulation requires three modifications to the traditional analysis of border irrigation. First, the geometry of the flow cross section must be described. Although furrows are not prismatic, the model results are not highly sensitive to changes in geometry and simple power functions can be used to relate depth of flow, area, hydraulic section, etc. The second factor added by furrow conditions is the need to utilize an infiltration equation incorporating both a time dependent rate and a basic or steady rate term (i.e., Kostiakov-Lewis) rather than a single time dependent rate term (i.e., Kostiakov). Advance can be simulated reasonably well without the addition of the basic intake rate term, but not runoff (5). Finally, infiltration is known to be affected by wetted perimeter and, thereby, flow rate (8). It is commonly assumed that infiltration is strictly a function of intake opportunity time, so its evaluation involves only one independent parameter (time). If it is also discharge dependent, it involves both an independent parameter and a dependent parameter (flow rate), thereby complicating the numerical solution. The model presented herein ignores this third factor without apparent loss of accuracy. As the mathematics of infiltration becomes better understood, this aspect of the model may be modified.

Cycled or surged irrigations (2,4,20) present additional complications in furrow flow simulation. Intermittent wetting of a furrow alters its hydraulic conductivity such that infiltration is not only time dependent, but also spatially dependent due to the stepwise advance of the wetted

[1]Prof., Agr. and Irrigation Engrg. Dept., Utah State Univ., Logan, Utah.
[2]Agr. Engr., Snake River Conservation Research Center, U.S. Dept. of Agr., Kimberly, Idaho.

Note.—Discussion open until May 1, 1984. To extend the closing date one month, a written request must be filed with the ASCE Manager of Technical and Professional Publications. The manuscript for this paper was submitted for review and possible publication on March 3, 1983. This paper is part of the *Journal of Irrigation and Drainage Engineering*, Vol. 109, No. 4, December, 1983. ©ASCE, ISSN 0733-9437/83/0004-0377/$01.00. Paper No. 18460.

region (13,21). Depending upon the prior wetting history at a particular point, the intake characteristics may vary substantially. This factor makes infiltration rates dependent on both intake opportunity time and spatial coordinates. The kinematic-wave model presented in this paper is the first with the capability of simulating furrow irrigation under surged flow.

Theoretical Model Development

The kinematic-wave model was initially developed for hydrologic applications (12,22), modified for sloping, free draining borders (3,18), and finally to sloping, free draining furrows (15,20). The model is a solution of the continuity equation,

$$\frac{\partial A}{\partial t} + \frac{\partial Q}{\partial x} + \frac{\partial Z}{\partial \tau} = 0 \quad \ldots\ldots (1)$$

with the assumption that discharge and cross-sectional area are uniquely related. In Eq. 1, A = the cross-sectional area (L^2); Q = the flow rate (L^3T^{-1}); Z = the infiltrated volume per unit length (L^2); t = time (T); x = distance (L); and τ = the intake opportunity time (T).

The area-discharge relation is generally provided by a uniform flow equation, which for this analysis is the Manning equation. Utilizing the empirical approximation for the squared hydraulic section proposed by Elliott, et al. (6)

$$(AR^{2/3})^2 = \rho_1 A^{\rho_2} \quad \ldots\ldots (2)$$

the Manning equation can be written (18) as

$$Q = \alpha A^m \quad \ldots\ldots (3)$$

The parameters in Eqs. 2–3 are defined as follows:

$$\alpha = \frac{(\rho_1 S_o)^{1/2}}{n} \quad \ldots\ldots (4)$$

$$\text{and} \quad m = \frac{\rho_2}{2} \quad \ldots\ldots (5)$$

in which ρ_1 and ρ_2 = empirical constants fitted to actual field furrow shape measurements; S_o = the furrow slope; and n = the Manning roughness coefficient. Eq. 3 can be substituted for Q in Eq. 1 to yield a continuity equation of one unknown dependent parameter, A. It is assumed that the spatial and temporal dependence of Z are defined.

Most of the kinematic-wave analyses to date have been characteristic solutions (3,15,18). Walker and Lee (20) utilized the first-order Lagrangian type integration presented by Strelkoff and Katapodes (19). In comparing the characteristic furrow model to the integral model, it was concluded that the integral model was superior on the basis of its adaptability to both surged and continuous flows, less sensitivity to the size of the time step, and the numerical stability of the solution.

Lagrangian integration was utilized in zero-inertia models to maximize the stability of the locally linearized numerical solution (6,19). The kinematic-wave model uses a Newton-Raphson solution which does not

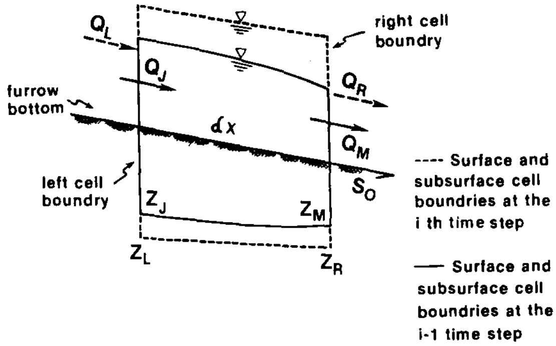

FIG. 1.—Kinematic-Wave Computational Cell (See Fig. 2 for Subscript Notation)

have the potential instability associated with the zero-inertia model. Consequently, simpler first-order Eulerian integration is used yielding an equivalent solution.

Integration of Eq. 1 is carried out over individual time and space increments (δt, δx) as follows (17):

$$\int_t^{t+\delta t}\left(\int_x^{x+\delta t}\frac{\partial Q}{\partial x}\,dx\right)dt+\int_x^{x+\delta t}\left(\int_t^{t+\delta t}\frac{\partial A}{\partial t}\,dt\right)dx$$

$$+\int_x^{x+\delta x}\left(\int_t^{t+\delta t}\frac{\partial Z}{\partial \tau}\,dt\right)dx=0 \quad \text{(6)}$$

The first-order result is

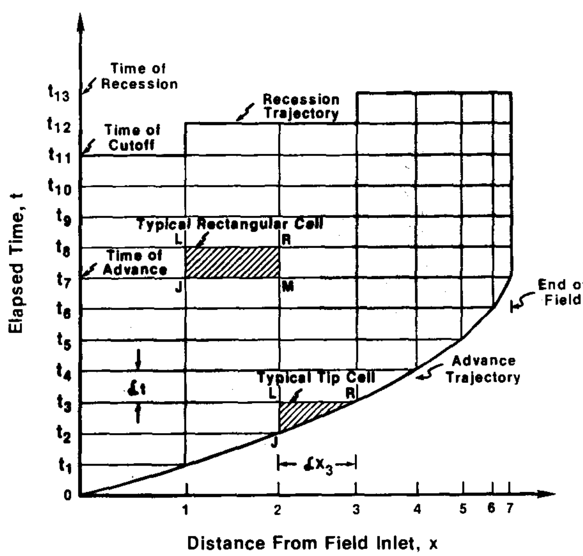

FIG. 2.—Time-Space Computation Grid

$$[\bar{Q}(x + \delta x, t) - \bar{Q}(x,t)]\delta t + [\tilde{A}(x, t + \delta t) - \tilde{A}(x,t)]\delta x$$
$$+ [\tilde{Z}(x, t + \delta t) - \tilde{Z}(x,t)]\delta x = 0 \quad \ldots\ldots (7)$$

The bar over the discharge variables indicates the time-averaged value over the δt interval, and the tilded A and Z variables are spatially averaged over the δx distance.

Eq. 7 can be shown as an incremental body of water within the flow system during a specific period as depicted in Fig. 1. Strelkoff and Katapodes (19) refer to the deforming body as a "cell" within the water body on and within the soil. The subscripts J, M, L, and R are used to distinguish which cell boundary is being considered (i.e., left, L, or right, R) and whether the time is the beginning, J, or ending, M, of the period (Fig. 2). Rewriting Eq. 7 in terms of the Fig. 1 notation yields

$$\{[\theta Q_R + (1 - \theta)Q_M] - [\theta Q_L + (1 - \theta)Q_J]\}\delta t + \{[\phi A_L + (1 - \phi)A_R]$$
$$- [\phi A_J + (1 - \phi)A_M]\}\delta x + \{[\phi Z_L + (1 - \phi)Z_R]$$
$$- [\phi Z_J + (1 - \phi)Z_M]\}\delta x = 0 \quad \ldots\ldots (8)$$

in which θ = the time averaging coefficient; and ϕ = the space averaging coefficient ($0 \leq \theta, \phi \leq 1$).

Numerical Solution

The solution to Eq. 1 is found by writing Eq. 8 for each cell or, equivalently, constructing the t-x grid, shown in Fig. 2, one time step at a time. In the physical sense, the flow profile expands at the advancing front by adding a new cell for each time step and then contracting from either end of the profile during recession. Along a particular time line, each grid cell is described by Eq. 8 in which only Q_R and A_R are unknown and can be reduced to simply A_R by Eq. 3. Solving for A_R gives

$$A_R^m + C_1 A_R + C_2 = 0 \quad \ldots\ldots (9)$$

$$\text{in which} \quad C_1 = \left(\frac{1 - \phi}{\theta\alpha}\right)\frac{\delta x}{\delta t} \quad \ldots\ldots (10)$$

$$\text{and} \quad C_2 = -A_L^m + \left(\frac{1 - \theta}{\theta}\right)\left(A_M^m - A_J^m\right) + \frac{\phi}{\theta\alpha}\left(A_L + Z_L - A_J - Z_J\right)\frac{\delta x}{\delta t}$$
$$+ \left(\frac{1 - \phi}{\theta\alpha}\right)(Z_R - A_M - Z_M)\frac{\delta x}{\delta t} \quad \ldots\ldots (11)$$

The left boundary condition provides the first value of the area at each time step and then the explicit solution moves to the right, cell-by-cell.

Initial Condition.—During the first time step, the flow advances the distance, δx_1. Variables A_R, A_J, A_M, and Z_R, Z_J, Z_M are zero, thereby reducing Eqs. 9–11 to

$$-A_L^m + \frac{\phi}{\theta\alpha}(A_L + Z_L)\frac{\delta x_1}{\delta t} = 0 \quad \ldots\ldots (12)$$

Since A_L is known for the inflow hydrograph, and Z_L is assumed uniquely

related to δt, the unknown incremental advance distance, δx_1, can be identified as

$$\delta x_1 = \frac{\theta \alpha A_L^m \delta t}{\phi(A_L + Z_L)} \quad \text{(13)}$$

The values of the time and space, θ and ϕ, averaging constants used in Eq. 13 are usually defined differently for the initial conditions and for the advancing tip right boundary condition than for the interior cells. In fact, a different ϕ value is used for A_L and Z_L in the denominator of Eq. 13 in most models (6,7,9,17,20). These "shape" or weighting factors have been given substantial consideration and theoretical derivation resulting in several analytical expressions. However, the writers believe the assumptions leading to these expressions [e.g., Elliott, et al. (6)] are inadequate. The weighting factor applied to the surface profile (multiplying A_L) assumes a uniform flow velocity behind the advancing tip. Initial advance increments using a 1–2 min time step may be as much as 20–30 m, and a uniform velocity is simply not observed. Second, the subsurface weighting factor (applied to Z_L) assumes the contribution to total infiltrated volume from the basic intake rate term in the Kostiakov-Lewis equation is negligible in comparison to the time dependent rate term. This is also inadequate in many soils. Consequently, for the model presented herein, Eq. 13 was used without distinguishing individual values for ϕ and θ for the various cells, and the analyses made to date have not shown a significant effect on model performance. Values θ and ϕ were both set equal to 0.65.

Boundary Conditions.—The left boundary is the field inlet with the following conditions:

$$A = Q = 0,\ t \leq 0; \quad A = A_o,\ Q_o = \alpha A_o^m,\ 0 < t \leq t_{co};$$

$$A = Q = 0,\ t > t_{co} \quad \text{(14)}$$

in which the zero subscript refers to the inflow hydrograph at $x = 0$; and t_{co} = the time of cutoff.

There are three possible right boundary conditions: (1) An advancing tip; (2) a free draining outflow; and (3) a diked downstream field boundary. Only the first two are considered in the kinematic-wave model. Eq. 13 is used for the advancing tip (Fig. 2). Following completion of the advance phase, the last downstream cell is evaluated as an interior cell, i.e., the flow leaves the field at normal depth.

Depletion and Recession.—The kinematic-wave model does not consider a depletion phase. As soon as the inflow is cutoff, the inlet area goes to zero during the time step. An artificial depletion phase can be added by inputting a decreasing hydrograph. However, in sloping furrows, the depletion phase is rarely longer than 1–2 min and can be neglected unless the field slope is very small.

Computations following the time of cutoff are the same as prior to cutoff. The flow area gradually declines at each point farther along the furrow length, eventually approaching zero. Recession is defined when the area at any station falls below 5% of the inlet flow area during the interval $0 < t < t_{co}$. The model predicts both left and right-side recession, as well as simultaneous left-side recession and right-side advance.

Modeling Surged Systems

A typical surge flow irrigation regime is shown in Fig. 3. Water applied to the furrow in a series of intermittent surges advances over a previously wetted furrow section and then over a dry section until recession is completed following the cutoff. Field and laboratory investigations (2,4,13,21) have documented that such a practice significantly reduces both the time dependent infiltration rates and the basic intake rates. Simulation of infiltration under surged conditions is based on the recirculating infiltrometer studies reported by Malano (13) and Walker, et al. (21), covering three soil types.

In a furrow section where the discharge is relatively constant from surge to surge, infiltration can be evaluated by two Kostiakov-Lewis equations:

$$Z_c = k\tau^a + f_o\tau \quad \ldots\ldots (15)$$

and $$Z_s = k'\tau^{a'} + f_o'\tau \quad \ldots\ldots (16)$$

in which Z_c and Z_s = the infiltrated volumes per unit of furrow length

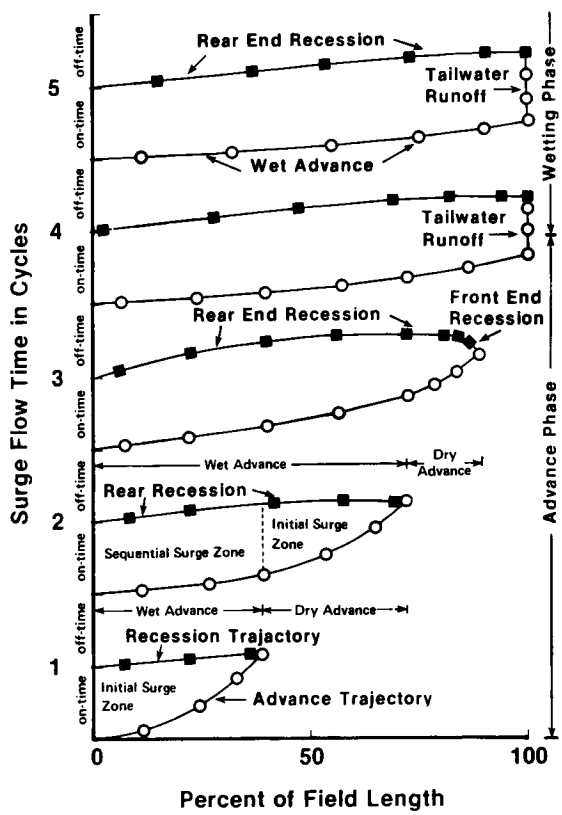

FIG. 3.—Characteristic Advance and Recession Curves for Surged Furrow Irrigation

(L^2) for dry, continuous flow conditions and wet, intermittent flow conditions, respectively. Parameters k, k', a, a', f_o and f_o' are the empirical parameters particular to the soil type and the effect of cycled wetting and drying. For Eq. 16, the intake opportunity time, τ, is cumulative, i.e., the sum of opportunity time over the number of surges applied.

Flow rate in a dry furrow section wetted by a surge is substantially lower than will occur in that section during succeeding surges. Field observations indicate, and Malano's (13) tests verify, that infiltration can be described by a function somewhere between Eqs. 15 and 16 for the second surge cycle. In the present version of the model, these changes are approximated using Eq. 15 for the dry sections, Eq. 16 for the third and succeeding surges, and a transition equation for the second surge.

TABLE 1.—Furrow Modeling Input Data for Continuous Flow

Model input parameters (1)	Flowell non-wheel furrow (2)	Flowell wheel furrow (3)	Kimberly non-wheel furrow (4)	Kimberly wheel furrow (5)	Benson 2-2-1 (6)	Printz 3-2-3 (7)	Matchett 2-3-5 (8)
Soil type	Sandy loam	Sandy loam	Silty-Clay loam	Silty-Clay loam	Clay loam	Loamy sand	Clay loam
Inflow, in liters per second	2.0	2.0	0.8	1.5	1.14	3.49	0.92
Field length, in meters	250	360	360	360	625	350	425
Field slope, in meters per meter	0.008	0.008	0.0104	0.0104	0.0044	0.0025	0.0095
Manning's n	0.04	0.04	0.04	0.04	0.02	0.02	0.02
Hydraulic section parameters							
ρ_1	0.3269	0.3269	0.6644	0.6644	0.58	0.615	1.35
ρ_2	2.734	2.734	2.8787	2.8787	2.91	2.924	3.00
Furrow geometry parameters[a]							
σ_1	0.782	0.782	0.962	0.962	1.05	1.07	2.18
σ_2	0.536	0.536	0.6046	0.6046	0.69	0.70	0.79
Time of cutoff, in minutes	350	400	400	200	613	110	1,364
Kostiakov-Lewis infiltration function parameters							
k, in cubic meters per meter per minute	0.002169	0.0028	0.00701	0.00884	0.018	0.01249	0.0033
a	0.673	0.534	0.533	0.212	0.02	0.024	0.400
f_o, in cubic meters per meter per minute	0.000222	0.00022	0.00017	0.00017	0.0001	0.000491	0.00003

[a]The furrow geometry expressed as depth = $\sigma_1 A \sigma_2$ are not used in the kinematic wave model but are included for use in other models.

Note: 1 m = 3.28 ft; 1 liter per second (lps).

TABLE 2.—Furrow Modeling Input Data for Surged Flow

Input parameters (1)	Flowell non-wheel furrow (2)	Flowell wheel furrow (3)	Kimberly non-wheel furrow (4)	Kimberly wheel furrow (5)
Soil type	Sandy loam	Sandy loam	Silty-Clay loam	Silty-Clay loam
Inflow, in liters per second	2.0	2.0	0.8	1.5
Field length, in meters	360	360	360	360
Field slope, in meters per meter	0.008	0.008	0.0104	0.0104
Manning's n	0.04	0.04	0.04	0.04
Hydraulic section parameters				
ρ_1	0.3269	0.3269	0.6644	0.6644
ρ_2	2.734	2.734	2.8787	2.8787
Furrow geometry parameters				
σ_1	0.782	0.782	0.962	0.962
σ_2	0.536	0.536	0.6046	0.6046
Continuous flow intake parameters				
k, in cubic meters per meter per minute	0.002169	0.00280	0.00701	0.00884
a	0.673	0.534	0.533	0.212
f_o, in cubic meters per meter per minute	0.000222	0.000222	0.00017	0.00017
Surge flow intake parameters				
k, in cubic meters per meter per minute	0.003561	0.00459	0.00494	0.00625
a	0.322	0.356	0.493	0.196
f_o, in cubic meters per meter per minute	0.00018	0.00018	0.00012	0.00012
Cycle time, in minutes	40	80	80, 120	80
Cycle ratio	0.5	0.5	0.5	0.5

Note: 1 m = 3.28 ft; 1 = liter per second (lps).

Letting $\bar{x}_{i-2}$ and $\bar{x}_{i-1}$ be the advance distances of the $i-2$ and $i-1$ surges, the transition function is written as

$$T = \left(\frac{\bar{x}_{i-1} - x}{\bar{x}_{i-1} - \bar{x}_{i-2}}\right)^{\lambda}, \quad \bar{x}_{i-2} \leq x \leq \bar{x}_{i-1}; \quad T = 0, \quad x < \bar{x}_{i-2} \quad \text{or} \quad x > \bar{x}_{i-1} \quad (17)$$

in which x = the location of the computational point of interest during the current time step, i; and λ = an empirical nonlinear distribution constant. Then the infiltration equation coefficients for the transition infiltration function are

$$k'' = k + (k - k')T \quad (18)$$

$$a'' = a + (a - a')T \quad (19)$$

and $$f_o'' = f_o + (f_o - f_o')T \quad (20)$$

In order to provide a nonlinear transition, values of λ in Eq. 17 can range from 2–5. A value of 3 was used in this paper and further tests are being conducted to determine if λ should be varied according to soil type and incremental surge advance.

Infiltration equations, such as Eq. 15, are based on cumulative opportunity time. The infiltrated volume added by a particular surge must therefore be computed as a difference. For instance, if at point x the opportunity time prior to the on-going surge is $\bar{\tau}$, and the opportunity time created by the present surge is τ, the infiltrated volume added during the present surge is

$$Z(t) = Z(\bar{\tau} + \tau) - Z(\bar{\tau}) \quad (21)$$

Verification and Analysis

To evaluate the model presented here, seven sets of continuous flow and four sets of surged flow test data, given in Tables 1–2, were eval-

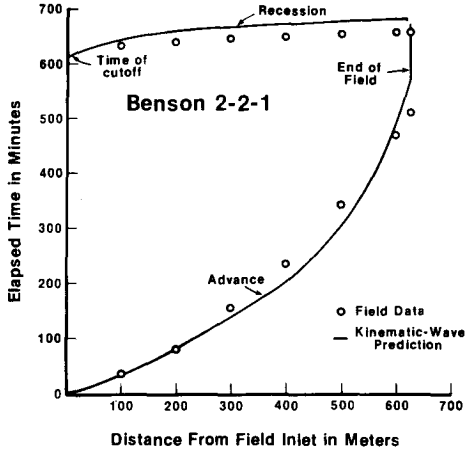

FIG. 4.—Analysis of Advance and Recession Using Benson 2-2-1 Test Data Reported by Elliott, et al. (6)

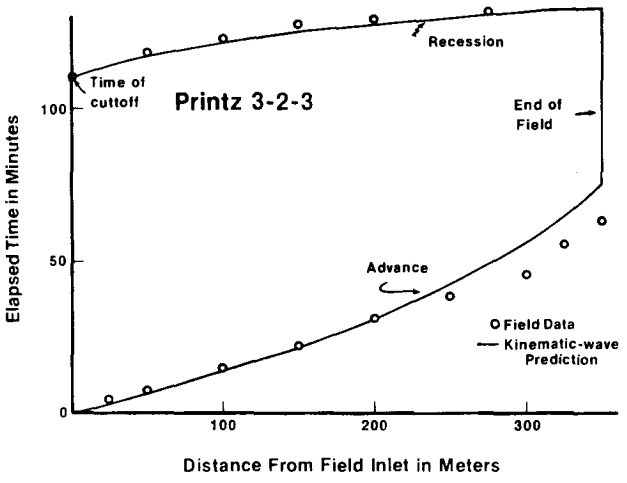

FIG. 5.—Comparison of Predicted and Measured Advance and Recession Trajectories, Printz 3-2-3 Test from Elliott, et al. (6)

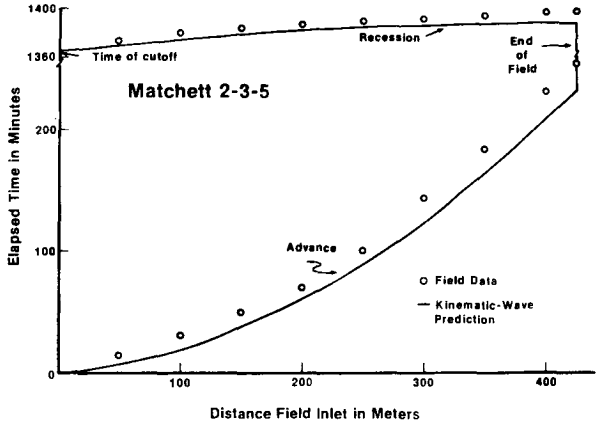

FIG. 6.—Analysis of Advance and Recession Data, Matchett 2-3-5 Test from Elliott, et al. (6)

uated. Although not all of these evaluations are reported herein, the entire data set is given for the benefit of other modelers who may wish to evaluate the same conditions.

Continuous Flow.—Continuous flow tests were conducted at three Colorado sites as reported by Elliott, et al. (6). Data from three of these, denoted Benson 2-2-1, Printz 3-2-3, and Matchett 2-3-5, were selected for evaluation in this paper. A comparison of the measured advance and recession trajectories with those predicted by the model are given in Figs. 4–6. The Colorado data represent a wide range of field conditions and the model adequately simulates each case; however, the Colorado data are not entirely independent. The values of k and a were computed from

advance data using the two-point volume balance solution presented by Elliott and Walker (5).

The four sets of data in Table 1, referenced as "Flowell" and "Kimberly," are representive data obtained from a series of tests conducted in Utah and Idaho. All of the parameters given are based on independent field measurements (13,14). The comparative model analysis of the wheel furrow tests are shown in Figs. 7–8. The predictions for the non-wheel furrows indicated essentially the same accuracy; however, neither non-wheel test completed the advance phase due to the higher intake rates.

Two results of general interest emerge from the continuous flow testing of the model. First, the calculated advance curves for the Colorado data are almost exactly the same as the zero-inertia predictions presented by Elliott, et al. (6). The kinematic-wave and zero-inertia model analyses of both continuous and surged flow at Kimberly and Flowell are also the same and will be reported in a future paper. Considering the range of field and soil conditions evaluated, it is concluded that unless field slopes are very flat with values of less than approximately 0.1%, the added complexity of the zero-inertia model is not necessary.

The second note of interest concerns recession. The model appears to deal adequately with the recession phase, although in relative terms the errors are occasionally large. Recession in a continuous flow regime is a very short process in sloping furrows and can generally be neglected since the contribution to soil moisture and runoff are usually small following cessation of the furrow inflow. Furrow simulation of the recession phase is markedly simpler than for border or basin irrigation analyses.

Surged Flow.—Cycled or surged irrigation tests were also conducted at Flowell, Utah, and Kimberly, Idaho. Fig. 9 shows the surge-by-surge advance and recession trajectories for a Flowell wheel furrow test. The results were similar for the other Flowell and Kimberly data. A combined kinematic-wave simulation for surge flow is shown in Fig. 10, with the actual and predicted surge advance front locations plotted. Three replications of the Flowell non-wheel furrow tests and two of the Kimberly non-wheel furrow tests are shown.

The second and third sets of Flowell data shown in Fig. 10 exhibit deviations of about 25% from the measured values for later surges. This can probably be attributed to the difficulty experienced in maintaining uniform discharge into the furrows, or variations in infiltration characteristics from one furrow to another.

In analyzing individual surge advance and recession trajectories from field measurements it is concluded that the spatial variability in soil intake properties has more impact on model performance for surge flow than for continuous flow conditions. The relatively simple approximations contained in Eqs. 17–20 provide a limited capability to deal with this problem, but have proved adequate in most cases. However, a substantial research effort is needed to clarify the infiltration processes for surged flow. In the interim, the kinematic-wave model should be adequate in most cases to describe the consequences of alternative surge flow practices and to indicate the potential advantage or disadvantage of a surge practice over a continuous flow regime.

The recession phase in surge flow is very important since a significant

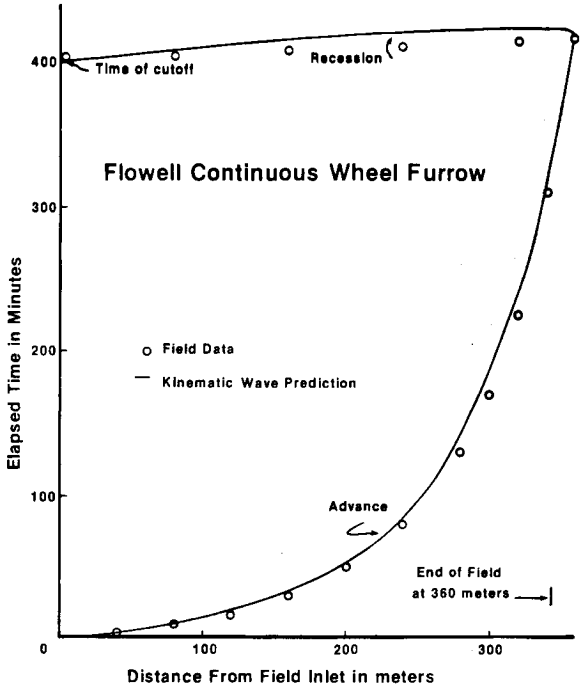

FIG. 7.—Comparison of Continuous Furrow Advance and Recession for Flowell Wheel Furrow

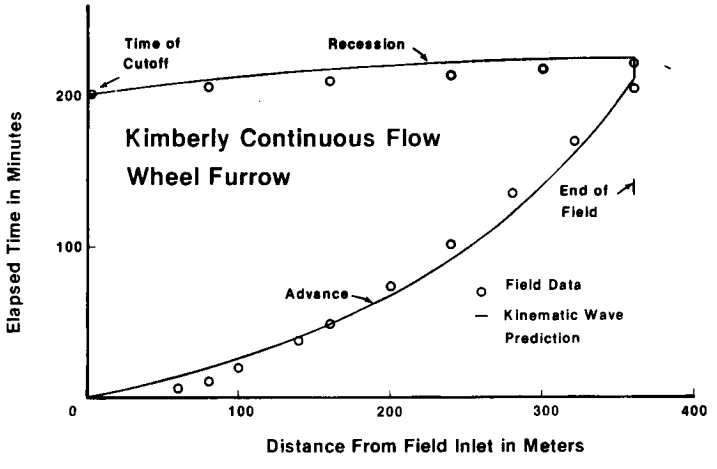

FIG. 8.—Model Analysis of Kimberly Continuous Wheel Furrow

fraction of the surge-to-surge extension of the field coverage actually occurs during this phase (i.e., simultaneous advance and recession). The kinematic-wave model evaluates this phase of the irrigation very well in the cases studied. However, recession is very difficult to monitor in the

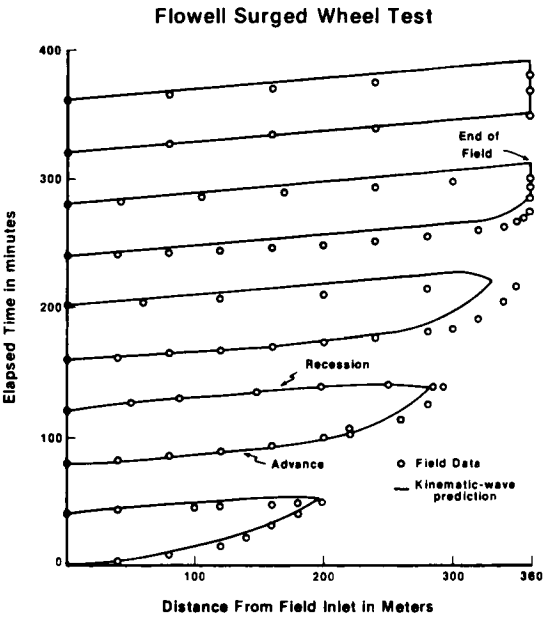

FIG. 9.—Measured and Predicted Advance Trajectories for 80-Minute Cycled Flow (40 minute ON-40 minute OFF) in Flowell Wheel Furrow

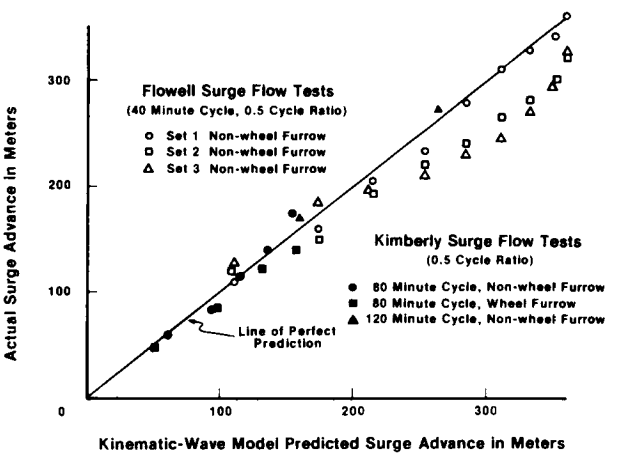

FIG. 10.—Comparison of Measured and Calculated Surge Advance Fronts for Kimberly and Flowell Tests (All Cycles Have Cycle Ratio of One-Half On, One-Half Off)

course of taking field measurements, and in sloping furrow systems the total process occurs in relatively short time periods. Under surged flow conditions, the model appeared to simulate field observations quite well, and particularly the extension of the wetted area during the recession phase.

Conclusions

Several important conclusions have emerged from this study. First, the kinematic-wave analysis should be a satisfactory tool to predict water advance, intake, and runoff for sloped furrow irrigated systems. Its accuracy is demonstrated with data encompassing a relatively wide range of field and soil conditions. It is simple to program and executes rapidly. The uniform flow assumption which was made to replace consideration of energy or momentum conservation appears basically sound in sloping furrows, including surged conditions where the Froude number of flows over previously wetted sections is higher. Finally, the emphasis of surface and subsurface profile shapes near the advancing front, given in the more complicated models, does not appear necessary in the kinematic-wave analysis. Indeed, these shape factors may be unrealistic even in the more detailed models when the time steps approach 1–2 min or more.

Describing infiltration under surged conditions and, therefore, simulating surge flow hydraulics, is admittedly in a preliminary stage. However, the simplistic approximations presented here yielded good results. Further research will improve this aspect of surface irrigation modeling, but it is concluded that it can be used in its present state to assist surge flow investigators, as well as those evaluating alternative design configurations.

The field data used in this paper are not completely sufficient to evaluate each assumption inherent in the kinematic-wave model. The observable variations in roughness and cross-sectional shape, for instance, can explain the deviations between predicted and measured advance and recession. A sensitivity analysis followed closely the results of several previous studies such as Elliott, et al. (6). It was therefore concluded that a comprehensive analysis of the model to determine parameter sensitivity and the model's limits of applicability should be based on comparisons with the hydrodynamic and zero-inertia solutions, a task yet to be undertaken.

Acknowledgments

Funding for this work was provided by the U.S. Department of Agriculture under Cooperative Agreement No. 58-9AHZ-573 and by the Utah Agricultural Experiment Station under Project No. AES 799.

Appendix I.—References

1. Bassett, D. L., "Mathematical Model of Water Advance in Border Irrigation," Transactions, American Society of Agricultural Engineers, Vol. 15, No. 5.1, 1972, pp. 992–995.

2. Bishop, A. A., Walker, W. R., Allen, N. L., and Poole, G. J., "Furrow Advance Rates Under Surge Flow Systems," *Journal of the Irrigation and Drainage Division*, ASCE, Vol. 107, No. IR3, Proc. Paper 16502, Sept., 1981, pp. 257–264.
3. Chen, C. L., "Surface Irrigation Using Kinematic-Wave Method," *Journal of the Irrigation and Drainage Division*, ASCE, Vol. 96, No. IR1, Proc. Paper 7134, Mar., 1970, pp. 39–46.
4. Coolidge, P. S., Walker, W. R., and Bishop, A. A., "Advance and Runoff-Surge Flow Furrow Irrigation," *Journal of the Irrigation and Drainage Division*, Vol. 108, No. IR1, Proc. Paper 16930, Mar., 1982, pp. 257–264.
5. Elliott, R. L., and Walker, W. R., "Field Evaluation of Furrow Infiltration and Advance Functions," Transactions, American Society of Agricultural Engineers, Vol. 25, No. 2, 1982, pp. 396–400.
6. Elliott, R. L., Walker, W. R., and Skogerboe, G. V., "Zero-Inertia Modeling of Furrow Irrigation Advance," *Journal of the Irrigation and Drainage Division*, ASCE, Vol. 108, No. IR3, Proc. Paper 17340, Sept., 1982, pp. 179–195.
7. Essafi, B., "A Recursive Volume Balance Model for Continuous and Surge Flow Irrigation," thesis presented to Utah State University at Logan, Utah, in 1982, in partial fulfillment of the requirements for the degree of Master of Science.
8. Fangmeier, D. D., and Ramsey, M. K., "Intake Characteristics of Irrigation Furrows," Transactions, American Society of Agricultural Engineers, Vol. 219, No. 4, 1978, pp. 696–700.
9. Katapodes, N. D., and Strelkoff, T., "Hydrodynamics of Border Irrigation—Complete Model," *Journal of the Irrigation and Drainage Division*, ASCE, Vol. 103, No. IR3, Proc. Paper 13188, Sept., 1977, pp. 309–324.
10. Kincaid, D. C., Heermann, D. F., and Kruse, E. G., "Hydrodynamics of Border Irrigation," Transactions, American Society of Agricultural Engineers, Vol. 15, No. 14, 1972, pp. 674–680.
11. Ley, T. W., "Sensitivity of Furrow Irrigation Performance to Field and Operation Variables," thesis presented to Colorado State University at Fort Collins, Colo., in 1978, in partial fulfillment of the requirements for the degree of Master of Science.
12. Lighthill, M. J., and Whitman, R. B., "On Kinematic Waves: I. Flood Movement in Long Rivers," *Proceedings of the Royal Society of London*, Series A, Vol. 229, 1955, pp. 201–316.
13. Malano, H. M., "Comparison of the Infiltration Process Under Continuous and Surge Flow," thesis presented to Utah State University at Logan, Utah, in partial fulfillment of the requirements for the degree of Master of Science.
14. Mostafazadehfard, B., "Furrow Geometry and Roughness Under Surge and Continuous Flow," thesis presented to Utah State University at Logan, Utah, in 1982, in partial fulfillment of the requirements for the degree of Master of Science.
15. Sherman, B., and Singh, V. P., "A Kinematic Model for Surface Irrigation: An Extension," *Water Resources Research*, Vol. 18, No. 3, June, 1982, pp. 659–667.
16. Singh, P., and Chauhan, H. S., "Shape Factors in Irrigation Water Advance Equation," *Journal of the Irrigation and Drainage Division*, ASCE, Vol. 98, No. IR3, Proc. Paper 9212, Sept., 1972, pp. 443–458.
17. Souza, F., "Non-linear Hydrodynamic Model of Furrow Irrigation," thesis presented to the University of California, at Davis, Calif., in 1981, in partial fulfillment of the requirements for the degree of Doctor of Philosophy.
18. Smith, R. E., "Border Irrigation Advance and Ephemeral Flood Waves," *Journal of the Irrigation and Drainage Division*, ASCE, Vol. 98, No. IR2, Proc. Paper 8979, June, 1972, pp. 289–305.
19. Strelkoff, T., and Katapodes, N. D., "Border-Irrigation Hydraulics with Zero Inertia," *Journal of the Irrigation and Drainage Division*, ASCE, Vol. 102, No. IR3, Proc. Paper 13189, Sept., 1977, pp. 325–342.
20. Walker, W. R., and Lee, T. S., "Kinematic-Wave Approximations of Surged

Furrow Advance," paper 81-2544, presented at the Dec. 15–18, 1981, American Society of Agricultural Engineers Winter Meeting, held at Chicago, Ill.
21. Walker, W. R., Malano, H., and Replogle, J. A., "Reduction in Infiltration Rates Due to Intermittent Wetting," paper 82-2029, presented at the June 27–30, 1982, American Society of Agricultural Engineers Summer Meeting, held at Madison, Wisc.
22. Woolhiser, D. A., and Liggett, J. A., "Unsteady, One Dimensional Flow Over a Plane—the Rising Hydrograph," *Water Resources Research*, Vol. 3, No. 3, 1967, pp. 753–771.

APPENDIX II.—NOTATION

The following symbols are used in this paper:

A = cross-sectional flow area, in square meters;
a = exponent in the Kostiakov-Lewis intake relation;
f_o = basic intake rate, in cubic meters per meter per minute;
k = constant in the Kostiakov-Lewis intake relation, in cubic meters per meter per minute;
m = exponent in the area-discharge relation;
n = Manning resistance coefficient;
Q = flow rate, in cubic meters per second;
R = hydraulic radius, in meters;
S_o = average field slope;
t = time, in minutes;
x = distance measured from field inlet, in meters;
Z = cumulative infiltration, in cubic meters per meter;
α = constant in area-discharge relation;
θ = space weighting factor;
λ = exponent to distribute surge flow infiltration effect;
ρ_1, ρ_2 = empirical parameters relating furrow depth and area;
σ_1, σ_2 = empirical parameters relating hydraulic section and area;
τ = intake opportunity time, in minutes; and
ϕ = time weighting factor.